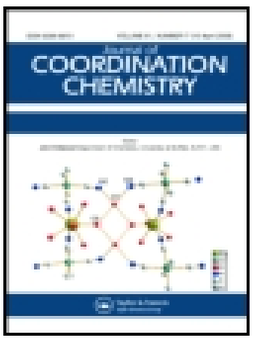

Journal of Coordination Chemistry

ISSN: 0095-8972 (Print) 1029-0389 (Online) Journal homepage: http://www.tandfonline.com/loi/gcoo20

New metal complexes with diclofenac containing 2-pyridineethanol or 2-pyridinepropanol: Synthesis, structural, spectroscopic, thermal properties, catechol oxidase and carbonic anhydrase activities

Sema Caglar, Esra Dilek, Bulent Caglar, Ekrem Adiguzel, Ersin Temel, Orhan Buyukgungor & Ahmet Tabak

To cite this article: Sema Caglar, Esra Dilek, Bulent Caglar, Ekrem Adiguzel, Ersin Temel, Orhan Buyukgungor & Ahmet Tabak (2016): New metal complexes with diclofenac containing 2-pyridineethanol or 2-pyridinepropanol: Synthesis, structural, spectroscopic, thermal properties, catechol oxidase and carbonic anhydrase activities, Journal of Coordination Chemistry, DOI: 10.1080/00958972.2016.1227802

To link to this article: http://dx.doi.org/10.1080/00958972.2016.1227802

Publisher: Taylor & Francis

Journal: *Journal of Coordination Chemistry*

DOI: http://dx.doi.org/10.1080/00958972.2016.1227802

New metal complexes with diclofenac containing 2-pyridineethanol or 2-pyridinepropanol: Synthesis, structural, spectroscopic, thermal properties, catechol oxidase and carbonic anhydrase activities

Sema Caglar†*, Esra Dilek‡, Bulent Caglar†, Ekrem Adiguzel†, Ersin Temel§, Orhan Buyukgungor¶, Ahmet Tabak

†*Department of Chemistry, Faculty of Arts and Sciences, Erzincan University, 24030, Erzincan, Turkey*
‡*Department of Biochemistry, Division of Pharmaceutical Basic Sciences, Faculty of Pharmacy, Erzincan University, 24030, Erzincan, Turkey*
§*Department of Electric and Energy, Technical Science Vocational High School,Giresun University, 28100,Giresun, Turkey*
¶*Department of Physics, Faculty of Arts and Sciences, Ondokuz Mayis University, 55200, Atakum, Samsun, Turkey*
Department of Chemistry, Faculty of Arts and Sciences, Sinop University, 57000 Sinop, Turkey

Abstract

Four new neutral diclofenac-based complexes, $[Co(dicl)_2(2\text{-pyet})_2]$ **1**, $[Ni(dicl)_2(2\text{-pyet})_2]$ **2,** $[Cu_2(dicl)_2(2\text{-pyet})_2]$ **3** and $[Cu_2(dicl)_2(2\text{-pypr})_2]$ **4** have been synthesized and characterized by elemental analysis, FT-IR, thermal analysis. Complexes **1**, **3** and **4** have also been characterized by X-ray single crystal structural analysis. The compounds of Co(II) and Ni(II) have octahedral geometry with two diclofenac and two 2-pyridineethanol ligands in the coordination sphere. The compounds of Cu(II) have square-pyramidal geometry and Cu(II) ions are linked via oxygens to the bridging 2-pyridineethanol or 2-pyridinepropanol ligands. The $\Delta\nu$ values acquired by FT-IR are in agreement with the single XRD data. Studies on the thermal properties are reported and the complexes are stable to 196, 216, 215 and 201^{o}C in

air, respectively. Two dinuclear Cu(II) complexes have demonstrated catalytic activity on oxidation of 3,5-di-*tert*-butylcatechol to 3,5-di-*tert*-butylquinone showing saturation kinetics at high substrate concentrations. The diclofenac complexes are investigated as inhibitors of the human cytosolic isoforms hCA I and II. The complexes are good as hCA I inhibitors (K_is of 1.52-55.06 μM) but only moderately efficient as hCA II inhibitors (K_is of 0.23-5.61 μM).

Keywords: Diclofenac; Crystal structure; FTIR; Catechol oxidation; Carbonic anhydrases

* Corresponding author. Tel.: +90 446 224 30 97 Fax: +90 446 224 30 16

E-mail address: semacaglar2002@hotmail.com (S. Caglar)

1. Introduction

Non-steroidal anti-inflammatory drugs (NSAIDs) form various chemical groupings: oxicams family such as meloxicam, piroxicam, tenoxicam and lornoxicam, and carboxylic acid family such as tolfenamic, diclofenac, mefenamic, flufenamic, ibuprofen and naproxen [1]. They are widely used as analgesics, anti-inflammatories, antipyretics and antitumor drugs [2-5]. The action of the NSAID is inhibition of cyclooxygenase (COX) production of prostaglandins [6]. Inhibition of COX also decreases prostaglandins in the epithelium of the stomach, making it more sensitive to corrosion by gastric acid.

Most anti-inflammatory drugs contain the carboxylate group. Carboxylates create an important class of ligands in inorganic and bioinorganic chemistry for metal-ligand interaction [7] with the ability to bind to metal ions in different ways (monodentate, bidentate or bridging) [8,9].

Diclofenac (dicl), 2-(2,6-dicholoroanilino)phenylacetic acid, belongs to the derivatives of phenylalkanoic acids. Dicl is widely used to treat pain, inflammatory disorders and acute migraines [8, 10-15]. Study of metal complexes with non-steroidal anti-inflammatory drugs as ligands is increasing. The crystal structures of metal(II) complexes with dicl have been

reported and biological evaluation of metal complexes were investigated [10, 15, 16-21]. It has been also reported that the metal complexes of some NSAIDs are better or have different pharmacological profile than free ligand [15-17, 22, 23]. Furthermore, these studies indicated that copper, manganese and nickel complexes showed enhanced biological properties and antioxidant activities compared to free Nadicl. [4, 10, 16].

Catechol oxidase enzyme exists widely in nature such as in plants, insects and crustaceans [24]. The crystal structures of catechol oxidase obtained from sweet potato shows that catechol oxidases present a dinuclear copper center in their active site and the copper center is surrounded by three histidines via three nitrogens [25-27]. The copper centers are bridged via hydroxyl groups in a trigonal pyramidal geometry. Therefore, mononuclear and dinuclear copper(II) complexes formed by oxygen bridge receive much attention [28-34]. This enzyme catalyzes the substrate specific oxidation of o-diphenols to o-diquinones in plants [35, 36].

Many of the enzymes found in living organisms are inhibited or activated with drugs. Inhibitions or activations of enzymes are important for the continuity of functions in living organisms. Carbonic anhydrases (CA; Carbonate hydrolyses, EC 4.2.1.1) are a family of metalloenzyme in mammals. These enzymes catalyze the conversion of CO_2 to HCO_3^- in cells. This conversion normally occurs very slowy. But they increase to reaction rate approximately 10^4-10^6 per second. By this reaction, they play important roles in several physiological/pathological processes such as electrolyte secretion, acid-base balance, bone resorption, respiration, carbon dioxide and ion transport, gluconeogenesis, ureagenesis and lipogenesis [37, 38]. Sixteen CA isozymes have been identified in mammals that differ in subcellular localization and catalytic activity [39]. Many such CA isozymes which assist these processes are important therapeutic targets with the potential to be inhibited/activated for the treatment of diseases such as glaucoma, edema, obesity, osteoporosis, epilepsy and cancer

[40-42]. Carbonic anhydrase inhibitors (CAI) are used in eye diseases, and have intraocular pressure lowering effects among the most potent drugs. Therefore, many scientists have focused on inhibitors of CA isozymes [43-47].

Inhibitory effects of different complexes, sulfonamide derivatives, anions, phenols, drugs,various chemicals and pesticides have been investigated against CA [21, 39, 43-52]. However, it is still important to discover further classes of potential CAIs in order to develop compounds with distinct inhibition profiles as compared to the known molecules [39, 43-46].

In the current study, we report the synthesis, structural and thermal characterization of metal(II) complexes with dicl in the presence of 2-pyridineethanol (2-pyet) or 2-pyridinepropanol (2-pypr). We also studied kinetics of the catalytic oxidation of 3,5-di-tert-butylcatechol ($DTBCH_2$) to 3,5-di-tert-butyl-1,2-benzoquinone (DTBQ) with dioxygen via spectrophotometric studies and CA inhibitory activities of the compounds were evaluated.

2. Experimental

2.1. Methods of sample characterization

$CoCl_2{\cdot}6H_2O$ (Sigma), $NiCl_2{\cdot}6H_2O$ (Sigma), $Cu(CH_3CO_2)_2{\cdot}H_2O$ (Sigma), sodium diclofenac (Sigma, 99.00%), 2-pyridineethanol (Aldrich, 98.00%), 2-pyridinepropanol (Aldrich, 96.00%) were used for the preparation of the complexes. FT-IR spectra of the complexes were recorded on a Thermo Nicolet 6700 spectrophotometer from 4000-450 cm^{-1} at 4 cm^{-1} resolution using KBr pellets. UV-Vis spectra were recorded on a PG 80+ from 200-1100 nm in DMF. Elemental analyses (C, H and N) of complexes were determined on a LECO CHNS-932 elemental analyzer. Thermal analysis runs were carried out on a PRIS Diamond TG/DTG/DTA apparatus from 30 to 1000 ^oC at a heating rate of 10 ^oC min^{-1} under dynamic air atmosphere (platinum crucibles and mass ~10 mg).

2.2. Synthesis of Complexes

2.2.1. $[Co(dicl)_2(2\text{-pyet})_2]$, 1

Nadicl (sodium diclofenac) (0.18 g, 0.6 mmol) and $CoCl_2 \cdot 6H_2O$ (0.06 g, 0.3 mmol) were dissolved in methanol (40 cm^3) with continuous stirring at 50 ^oC. Then 2-pyet (0.07 g, 0.6 mmol) was added. The solution was left for slow evaporation at room temperature and X-ray quality purple crystals appeared after five days. The purple crystals were filtered, washed with water and dried at room temperature.

Yield for **1**: 78 %; Analytical data for [$C_{42}H_{38}Cl_4N_4O_6Co$]: Found: C, 56.32; H, 4.23; N, 6.31 %; calcd: C, 56.28; H, 4.24; N, 6.25 %).

2.2.2. [Ni(dicl)$_2$(2-pyet)$_2$], 2

Complex **2** was prepared in a similar way to **1** with the use of $NiCl_2 \cdot 6H_2O$ (0.06 g, 0.3 mmol) instead of $CoCl_2 \cdot 6H_2O$. The resulting solution was left for slow evaporation at room temperature and green micro crystals appeared after one week. The green micro crystalline product was filtered, washed with water and dried at room temperature.

Yield for **2**: 89 %; Analytical data for [$C_{42}H_{38}Cl_4N_4O_6Ni$]: Found: C, 56.32; H, 4.23; N, 6.31 %; calcd: C, 56.29; H, 4.24; N, 6.25 %).

2.2.3. [Cu$_2$(dicl)$_2$(2-pyet)$_2$], 3

$Cu(CH_3CO_2)_2 \cdot H_2O$ (0.06 g, 0.3 mmol) and Nadicl ligand (0.18 g, 0.6 mmol) were dissolved in methanol (40 cm^3) with continuous stirring at 50 ^oC. Then 2-pyet (0.07 g, 0.6 mmol) was added. The resulting solution was left for slow evaporation at room temperature, giving blue crystals after four days. The formed crystals were filtered, washed with water and dried at room temperature.

Yield for **3**: 91 %; Analytical data for [$C_{42}H_{36}Cl_4N_4O_6Cu_2$]: Found: C, 52.40; H, 3.78; N, 5.80 %; calcd: C, 52.15; H, 3.74; N, 5.82 %).

2.2.4. [Cu$_2$(dicl)$_2$(2-pypr)$_2$], 4

Complex **4** was synthesized in a similar way to **3** with the use of 2-pypr (0.08 g, 0.6 mmol) instead of 2-pyet. The resulting solution was left for slow evaporation at room

temperature and X-ray quality blue crystals appeared after two weeks. The formed crystals were filtered, washed with water and dried at room temperature.

Yield for **4**: 84 %; Analytical data for [$C_{44}H_{40}Cl_4N_4O_6Cu_2$]: Found: C, 53.28; H, 4.20; N, 5.61 %; calcd: C, 53.34; H, 4.04; N, 5.65 %).

2.3. X-ray crystallography

The diffraction data were collected on a STOE IPDSII image plate detector using Mo Kα radiation (α= 0.71073Å, T = 293 K). A summary of the key crystallographic information is given in Table 1. Data collection: Stoe X-AREA [53]. Cell refinement: Stoe X-AREA [53]. Data reduction: Stoe X-RED [54]. The structure was solved by direct-methods using SHELXS-97 [54] and anisotropic displacement parameters were applied to non-hydrogen atoms in a full-matrix least-squares refinement based on F_2 using SHELXL-97 [54]. All hydrogens attached to carbon were positioned geometrically and refined by a riding model with U_{iso} 1.2 times than that of attached atoms and remaining hydrogens were located from the Fourier difference map.

2.4. Catechol oxidase activity

The catecholase activities of **3** and **4** were evaluated by reaction with 3,5-di-tert-butylcatechol at 25 ^{o}C in DMF. The absorption at 395 nm, characteristic of the formed 3,5-di-tert-butylquinone (DTBQ), was measured as a function of time. The initial reaction rate was determined from the slope of the trace at 395 nm in the first minute of the reaction. For this purpose seven different ratios of complex and substrate were studied [20]. The minimum complex to substrate ratio was 1:5 and the maximum complex to substrate ratio was 1:50. Copper(II) complexes exhibited saturation kinetics. The data satisfied the Michaelis-Menten equation; K_m, V_{max}, and k_{cat} values were determined from Lineweaver-Burk plots.

2.5. Purification and enzymatic activity of hCA I and hCA II

The CA isozymes have been purified many times from different organisms [43, 45, 51, 52, 55, 56]. In this study, the purification of the two CA isozymes was performed with a simple one step method by a Sepharose-4B-tyrosine-sulfanilamide affinity column from human erythrocytes [45, 47]. Then the activity of hCA I and hCA II were determined by using the esterase activity method with 4-nitrophenyl acetate (NPA) as substrate [45]. The inhibitory effects of the diclofenac complexes were tested *in vitro*. The inhibitor concentrations that caused 50% inhibition (IC_{50}) were determined from % activity versus [Inhibitor] plots and the K_i values were calculated from Lineweaver-Burk plots [20].

2.6. Protein determination

Bradford method was used to carry out quantitative protein assay. Sodium dodecyl sulfate-polyacrylamide gel electrophoresis (SDS-PAGE) was performed after purification of the enzymes according to the Laemmli's procedure as in previous studies [45, 57-58]. Samples were applied as 20 µg to the electrophoresis. Gels were smudged for 1.5 h in 0.1% Coomassie Brilliant Blue R-250 in 50% methanol and 10% acetic acid, then stored in the same solvent without dye.

3. Results and discussion

3.1. FT-IR Spectra

In all complexes, the stretching vibrations of N-H are at 3266, 3270, 3247 and 3232 cm^{-1}, respectively. This band is at 3250 cm^{-1} in Nadicl. The aromatic and aliphatic C-H stretching bands of Nadicl, 2-pyridineethanol and 2-pyridinepropanol ligands are 3071-2857 cm^{-1}.

In $[Co(dicl)_2(2\text{-}pyet)_2]$, $[Ni(dicl)_2(2\text{-}pyet)_2]$, $[Cu_2(dicl)_2(2\text{-}pyet)_2]$ and $[Cu_2(dicl)_2(2\text{-}pypr)_2]$, the $\nu_{asym}(COO)$ band is at 1572, 1572, 1577 and 1574 cm^{-1} and the $\nu_{sym}(COO)$ at 1368, 1369, 1452 and 1449 cm^{-1}, respectively. The ligands which are included in carboxylate groups have two donor sites and coordinate to metal ions with carboxyl oxygens. The

coordination mode of the carboxylate groups can be determined from IR spectra by comparing the Δv [v_{asym}(COO) - v_{sym}(COO)] value. The Δv [v_{asym}(COO) - v_{sym}(COO)] values are 204, 203, 120 and 125 cm^{-1}, respectively. The position of these bands suggest monodentate for **1** and **2** and bidentate for **3** and **4** [59-60].

When 2-pyet or 2-pypr was bound to metal via nitrogen of pyridine ring, the pyridine ring vibration of free 2-pyet or 2-pypr at 1592 and 1423 cm^{-1} shift to higher frequencies. In the IR spectra of **1**-**4**, these peaks exist at 1603 and 1453 cm^{-1}. The medium intensity bands at 1307-1303 cm^{-1} and 1232-1249 cm^{-1} belong to the anti-symmetric and symmetric stretching ν(C-N-C) of dicl ligand, respectively. The band attributed to in plane deformation of the C-H groups occurs at 940 cm^{-1}. The bands at 780 cm^{-1} correspond to ν(C-Cl) vibration of dicl. The bands at 600-450 cm^{-1} are attributed to metal-oxygen and metal-nitrogen stretching vibrations.

3.2. Crystal Structures

3.2.1. $[Co(dicl)_2(2\text{-pyet})_2]$ 1

Fig.1 shows an ORTEP with the labelling scheme. Selected bond distances and angles are found in Table 2. The single crystal X-ray analysis shows that $[Co(dicl)_2(2\text{-pyet})_2]$, **1**, is neutral and crystallizes in monoclinic space group P21/c.

The six coordinate Co(II) has slightly distorted octahedral geometry with two carboxylate oxygens, O(2) and O(2^i) coming from the two dicl ligands and two nitrogens and two ethanoic oxygens (N(1) and N(1^i); O(1) and O(1^i)) coming from the two 2-pyet ligands. 2-Pyet is bidentate forming a six-membered chelating ring with cobalt. Intramolecular O-H···O, N-H···O and C-H···O type hydrogen bonds generate S(6), S(7) and S(6) rings, respectively. The hydrogen bonding and intermolecular interactions are given in Table 3. Intermolecular π···π interactions form a 2-D supramolecular structure parallel to the bc-plane (Fig. 2).

Co-O_{dicl} bond distance is 2.0934(13) Å, which is similar with corresponding values in $[Co(dicl)_2(2\text{-aepyr})_2]$ (2.077(2)-2.095 Å) [21]. The Co-O_{dicl} bond distance is slightly shorter than the 2.080(2)-2.228(2) Å found in $[Co(dicl)_2(3\text{-pic})_2]$ [21], where 2-aepyr, 3-pic are 1-(2-aminoethyl)pyrrolidine and 3-picoline.

3.2.2. $[Cu_2(dicl)_2(2\text{-pyet})_2]$ 3 and $[Cu_2(dicl)_2(2\text{-pypr})_2]$ 4

The ORTEP viewes of the asymmetric units of **3** and **4**, along with the atomic numbering scheme, are shown in Fig. 3 and 5, respectively. Selected bond lengths and angles together with the hydrogen bonding geometries are given in Tables 2 and 3. Complexes crystallize in monoclinic space group P21/c. The Cu(II) is formed by $CuNO_4$ group with approximate square pyramidal geometry. The structural distortion index tau (τ) was calculated as 0.12 for **3**; 0.30 for **4** and the τ-value is appropriate for square-pyramidal geometry.

Cu(II) ions are linked via oxygens to the bridging ligands (2-pyet for **3**; 2-pypr for **4**) and 2-pyet or 2-pypr is also connected to each metal ion through the nitrogen. The five coordinate geometry of each Cu(II) is brought about by ligation of the metal by a dicl as the second ligand. In **3**, intramolecular N-H···O type hydrogen bonds generate S(7) rings. Intermolecular C-H···π interactions form a riband of edge-fused $R_2^2(22)$ rings running through the b-axis. In **4**, intramolecular N-H···O type hydorgen bonds generate S(7) rings. Intermolecular C-Cl···π interactions form a 2-D supramolecular structure parallel to bc-plane. C-H···π, C-Cl···π and hydrogen bonding interactions of **3** and **4** are shown in Fig. 4 and 6, respectively.

Cu-O_{dicl} bond distance is 1.921(2) Å for **3** and 1.924(2) Å for **4**, which is shorter than the 1.966(5)-2.609(6) Å found in $[Cu(dicl)_2(3\text{-pic})_2]$ [20] and in $[Cu(dicl)_2(4\text{-pic})_2]$ (1.941(2)-2.1934(2) Å) [20]. Cu-O_{dicl} bond distance is similar with a corresponding values in $[Cu(dicl)_2(py)_2]$ (1.9446(15) Å) [61].

3.3. Thermal Analyses

Thermal gravimetric analyses are used to analyze the thermal stabilities of **1**-**4**. The results demonstrate that the complexes are stable to ~ 200 ^{o}C in air. Complex **1** decomposes in two steps. The first step between 30-203 ^{o}C corresponds to the loss of one coordinated 2-pyet with the endothermic DTA signal at 192 ^{o}C ($DTG_{max.}$ = 196 ^{o}C, found 14.20%, calc. 13.75%). The second stage contains a major mass loss extending from 203 °C to 687 °C, suggesting decomposition of one 2-pyet and two dicl ligands with a mass loss of 77.1% (DTG_{max} = 279°C, calc. 79.66%). The final weight of residue observed as 8.7% (calc. 8.36%) can be attributed to the CoO.

For **2**, the endothermic peak of DTA (223 °C) curve from 30-261 °C is related to loss of two 2-pyet ligands (DTG_{max} = 216, 226 °C; found 26.20%; calc. 27.51%). The second stage between 261-436 °C corresponds to the release of one dicl ligand by giving an exothermic peak (DTG_{max} = 292 °C; found 32.80%; calc. 32.96%). The last stage involves decomposition of one dicl (DTG_{max} = 516 °C; found 32.49%; calc. 32.96%). The final decomposition product is NiO (found = 8.51%, calc. = 8.34%).

Complex **3** shows three steps of decomposition. The first stage between 30 and 227 ^{o}C is related to removal of two 2-pyet ligands (DTG_{max} = 215 °C; DTA = 212 °C; found 25.20%; calc. 25.56%). The second stage from 227-557 °C is assigned to decomposition of one dicl ligand, observed mass loss 31.30% (DTG_{max} = 329 °C, DTA = 360 °C (exo) calc. 30.63%). The third stage weight loss of 28.9% between 557 and 780 °C corresponds to loss of one dicl ligand (calcd. 30.63%). The end products can be assigned to CuO by considering calculated mass (14.6%) and found weights (16.49%).

For **4**, the first peak between 30 and 228 °C is related to removal of two 2-pypr ligands (DTG_{max} = 201, 209 °C; DTA = 199 (endo) °C; found 26.66%; calc. 27.66%). In the second stage, exothermic degradation of one dicl occurs at 228-477 ^{o}C with exothermic DTA peaks at 321 and 343 ^{o}C (found 30.24%; calc. 29.76%). The next stage, from 477-650 ^{o}C, corresponds

to loss of one dicl ligand (found 27.65%; calc. 29.76%). The final decomposition product is CuO (found 15.45%; calc. 16.03%).

3.4. Catechol oxidase activity

The oxidase biomimetic catalytic reactivity of the reported dinuclear copper complexes (**3** and **4**) towards the aerobic oxidation of $DTBCH_2$ under catalytic conditions was studied using a UV-Vis spectrophotometer by following the appearance of the absorption maximum of quinone at 395 nm.

In order to determine the catechol oxidase activity of the dinuclear copper complexes, 10^{-4} M solutions of **3** and **4** in DMF were treated with 50 equiv. of $DTBCH_2$ under aerobic conditions at room temperature. Time-dependent increases in quinone absorbance were examined at 300-600 nm. In this study, 10^{-4} M complex and 5×10^{-3} M substrate were stirred at equal volumes and quinone formation was determined by UV-Vis spectrophotometer at 395 nm. A blank experiment without catalyst did not show formation of the quinone up to 3 h in DMF. Kinetic measurements were made spectrophotometrically on a UV-Vis spectrophotometer, following the appearance of DTBQ (395 nm absorbance maximum, $\varepsilon = 1621$ $Lmol^{-1}cm^{-1}$ in DMF). The kinetic experiments were conducted at 25 °C. The rate determining step was found to change with the substrate to complex ratio. While the complex concentrations were kept constant ($1x10^{-4}$ M), substrate concentration was changed (50-40-30-20-15-10-$5x10^{-4}$ M). At least three runs were taken for each concentration and the initial rates were determined from the slope of the tangent to the absorbance vs time curve at $t = 0$ (Fig. 7).

Turnover number (k_{cat}), Michaelis-Menten constant (K_M) and maximum velocity (V_{max}) can be calculated by means of Lineweaver-Burk plot. The V_{max} values are $2.06x10^{-6}$ and $1.87x10^{-6}$ Ms^{-1}; K_M values $7x10^{-4}$ and $2.32x10^{-4}$ M; k_{cat} values are 148.10 and 135.24 h^{-1} for **3** and **4**, respectively. The k_{cat} values for **3** and **4** have been compared with

reported dinuclear copper(II) complexes [62-66]. Our result is quite comparable with literature, but much lower than that of the native enzyme catechol oxidase isolated from sweet potatoes (Ipomoea batatas) (K_{cat} = 8.25x10^6 h^{-1}) [67].

3.5. Carbonic Anhydrase Activity Assay

We synthesized four diclofenac complexes and evaluated their ability to inhibit hCA I and hCA II over a wide range of concentrations (0.1–100 μM). IC_{50} values were determined for the in vitro inhibition of hCA I and hCA II with the complexes, by the esterase method with 4-NPA as substrate. These results are given in Table 4. Complexes **1**-**4** showed in vitro inhibitory effects on hCA I and hCA II. **3** had the strongest inhibitory effects on hCA I and hCA II. Inhibition types and K_i values were determined for the complexes using Lineweaver-Burk curves for hCA I and hCA II (Fig. 8 and 9). **1** and **3** acted as uncompetitive inhibitors with 4-NPA as substrate, **2** and **4** acted as noncompetitive inhibitors for hCA I. **1** and **2** acted as uncompetitive inhibitors with 4-NPA as substrate, **3** and **4** acted as noncompetitive inhibitors for hCA II. These complexes showed inhibition constants in the range of 1.52-55.06 μM for hCA I and 0.23-5.61 μM for hCA II (Table 5). **1-4** showed more inhibitory effect compared to the our previously reported Co(II) / Ni(II)-diclofenac complexes [21]. This situtation indicated that the type of N-donor heterocyclic ligands affected the carbonic anhydrase activity. In addition these complexes exhibited significant inhibition at low concentration. Interaction of most CA isozymes with several types of phenols, such as simple phenol and its substituted derivatives, clioquinol, salicyclates, some of their derivatives and complexes derived from drugs has been investigated [21, 45, 50, 68].

4. Conclusions

The synthesis and characterization of the mononuclear cobalt(II), nickel(II) and dinuclear copper(II) complexes with the non-steroidal anti-inflammatory drug diclofenac in the presence of 2-pyridineethanol or 2-pyridinepropanol have been reported. Diclofenac is

bound to metal(II) ions via carboxylate oxygens. This coordination mode is supported with X-ray diffraction data and FT-IR spectral results. The purity of the complexes was confirmed by elemental analysis data. Thermal analysis data and characteristic IR vibrational bands of **1** were similar to those obtained for **2**. These results demonstrated that **1** and **2** have similar coordination mode and crystal structure. Structurally characterized $[Co(dicl)_2(2\text{-pyet})_2]$ and $[Ni(dicl)_2(2\text{-pyet})_2]$ have distorted octahedral geometry; $[Cu_2(dicl)_2(2\text{-pyet})_2]$ and $[Cu_2(dicl)_2(2\text{-pypr})_2]$ have square pyramidal geometry. Complexes are stable to approximately 200^{o}C. Catechol oxidase activities of copper complexes have been investigated by using $DTBCH_2$ as substrate in DMF. **3** and **4** showed good catechol oxidase activity. The diclofenac complexes represent a different class of hCA I and hCA II, and the results discussed in this study may help design new analogs with enhanced activity. Furthermore, similar metal complexes by preparing the NSAID and/or by adding mixed-atom donors as co-ligands could be synthesized and characterized.

5. Supplementary Material

Supplementary data CCDC-1440607, 1440608 and 1440609 contains the supplementary crystallographic data for complex **1, 3** and **4** respectively. These data can be obtained free of charge via http://www.ccdc.cam.ac.uk/conts/retrieving.html, or from the Cambridge Crystallographic Data Centre, 12 Union Road, Cambridge CB2 1EZ, UK; fax: (+44) 1223-336-033; or e-mail: deposit@ccdc.cam.ac.uk.

Acknowledgement

The Research Foundation of Erzincan University is acknowledged for the financial support to this work under the Project Number 110205.

Disclosure statement

No potential conflict of interest was reported by the authors.

References

[1] J.E. Weder, C.T. Dillon, T.W. Hambley, B.J. Kennedy, P.A. Lay, J.R. Biffin, H.L.Regtop, N.M. Davies. *Coord. Chem. Rev*., **232**, 95 (2002).

[2] C.P. Duffy, C.J. Elliott, R.A. O'Connor, M.M. Heenan, S. Coyle, I.M. Cleary, K. Kavanagh, S. Verhaegen, C.M. O'Loughlin, R. NicAmhlaoibh, M. Clynes. *Eur. J. Cancer*., **34,** 1250 (1998).

[3] A. Zianna, M. S. Ristovic, G. Psomas, A. Hatzidimitriou, E. Coutouli-Argyropoulou, M. Lalia-Kantouri. *J. Coord. Chem*., 68, 4444 (2015).

[4] M. Zampakou, A. G. Hatzidimitriou, A. N. Papadopoulos, G. Psomas. *J. Coord. Chem*., 68, 4355 (2015).

[5] J.I. Johnsen, M. Lindskog, F. Ponthan, I. Pettersen, L. Elfman, A. Orrego, B. Sveinbjornsson, P. Kogner. *Cancer Lett*., **228,** 195 (2005).

[6] A.R. Amin, P. Vyas, M. Attur, J. Leszczynskapiziak, I.R. Patel, G. Weissmann, S.B. Abramson. *Proc. Natl. Acad. Sci*., **92**, 7926 (1995).

[7] J.R.J. Sorenson, in: H. Sigel, (Ed.), Metal Ions in Biological Systems, vol. 14, Marcel Dekker, New York, 1982, pp. 77.

[8] S.B. Etcheverry, D.A. Barrio, A.M. Cortizo, P.A.M. Williams. *J. Inorg. Biochem*., **88**, 94 (2002).

[9] I.M. Pereira e Silva, D. de Moraes Profirio, R.E. Ferraz de Paiva, M. Lancellotti, A.L.B. Formiga, P.P. Corbi. *J. Mol. Struct*., **1049**, 1 (2013).

[10] M. Kyropoulou, C.P. Raptopoulou, V. Psycharis, G. Psomas. *Polyhedron*, **61**, 126 (2013).

[11] A. Quirinia, A. Viidik, S.J. Plast. *Reconstr. Hand Surg*., **31**, 213 (1997).

[12] J.N. Housby, C.M. Cahill, B. Chu, R. Prevelige, K. Bickford, M.A. Stevenson, S.K. Calderwood. *Cytokine*, **11**, 347 (1999).

[13] A. Beck, G. Krischak, T. Sorg, P. Augat, K. Farker, U. Merkel, L. Kinzl, L. Claes. *Arch. Orthop. Trauma. Su.*, **123**, 327 (2003).

[14] M. Tunçay, S. Çaliş, H.S. Kaş, M.T. Ercan, I. Peksoy, A.A. Hincal. *Int. J. Pharm.*, **195**, 179 (2000).

[15] D. Kovala-Demertzi, D. Mentzafos, A. Terzis. *Polyhedron*, **12**, 1361 (1993).

[16] F. Dimiza, F. Perdih, V. Tangoulis, I. Turel, D.P. Kessissoglou, G. Psomas. *J.Inorg. Biochem.*, **105(3)**, 476 (2011).

[17] D. Kovala-Demertzi, A. Theodorou, M.A. Demertzis, C.P. Raptopoulou, A. Terzis. *J. Inorg. Biochem.*, **65**, 151 (1997).

[18] C. Castellari, G. Feroci, S. Ottani. *Acta Crystallogr. Sect. C.*, **55**, 907 (1999)..

[19] N. Kourkoumelis, M.A. Demertzis, D. Kovala-Demertzi, A. Koutsodimou, A. Moukarika, *Spectrochim. Acta, Part A.*, **60**, 2253 (2004).

[20] S. Caglar, I.E. Aydemir, E. Adıgüzel, B. Caglar, S. Demir, O. Buyukgungor. *Inorg. Chim. Acta.*, **408**, 131 (2013).

[21] S. Caglar, I.E. Aydemir, M. Cankaya, M. Kuzucu, E. Temel, O. Buyukgungor. *J. Coord. Chem.*, **67**, 969 (2014).

[22] G. Crisponi, V.M. Nurchi, D. Fanni, C. Gerosa, S. Nemolato, G. Faa. *Coord. Chem. Rev.*, **254**, 876 (2010).

[23] J.A. Drewry, P.T. Gunning. *Coord. Chem. Rev.*, **255**, 459 (2011).

[24] A.L. Hughes. *Immunogenetics*, **49**, 106 (1999).

[25] T. Klabunde, C. Eicken, J.C. Sacchettini, B. Krebs. *Nat. Struct. Biol.*, **5**, 1084 (1998).

[26] R. Than, A.A. Feldman, B. Krebs. *Coord. Chem. Rev.*, **182**, 211 (1999).

[27] C. Gerdemann, C. Eicken, B. Krebs. *Acc. Chem. Res.*, **35**, 183 (2002).

[28] G. Speier. *J. Mol. Catal.*, **37**, 259 (1986).

[29] D. M. Boghaei, M. Gharagozlou, M. Sayadi. *J. Coord. Chem.*, **60**, 2283 (2007).

[30] E. Monzani, L. Quinti, A. Perotti, L. Casella, M. Gullotti, L. Randaccio, S. Geremia, G. Nardin, P. Faleschini, G. Tabbı. *Inorg. Chem.*, **37**, 553 (1998).

[31] A. E. M. M. Ramadan, M. M. Ibrahim, I. M. El-Mehasseb, *J. Coord. Chem.*, **65**, 2256 (2012).

[32] S.Y. Shaban, A.M. Ramadan, R. van Eldik. *J. Coord. Chem.*, **65**, 2415 (2012).

[33] S. Caglar, E. Adiguzel, B. Sariboga, E. Temel, O. Buyukgungor. *J. Coord. Chem.*, **67**, 670 (2014).

[34] Z.F. Chen, Z.-R. Liao, D.-F. Li, W.-K. Li, X.-G. Meng. *J. Inorg. Biochem.*, **98**, 1315 (2004).

[35] B. Salvato, M. Santamaria, M. Beltramini, G. Alzuet, L. Casella. Biochemistry, **37**, 14065 (1998).

[36] R. Bakshi, M. Rossi, F. Caruso, P. Mathur. *Inorg. Chim. Acta*, **376**, 175 (2011).

[37] C.T. Supuran. *Nat. Rev. Drug Discov.*, **7**, 168 (2008).

[38] N. Korkmaz, O.A. Obaidi, M. Senturk, D. Astley, D. Ekinci and C.T. Supuran. *J. Enzym. Inhib. Med. Chem.*, **30**, 75 (2015).

[39] Y. Akbaba, H.T. Balaydın,A. Menzek, S. Göksu, E. Şahin, D. Ekinci. *Arch. Pharm.*, **346(6)**, 447 (2013).

[40] C.T. Supuran, D. Vullo, G. Manole, A. Casini, A. Scozzafava. *Cardiovasc Hematol Agents Med. Chem.*, **2**, 49 (2004).

[41] S.K. Nair, P.A. Ludwig, D.W. Christianson. *J. Amer. Chem. Soc.*, **116**, 3659 (1994).

[42] J.R. Casey. *Biochem. Cell Biol.*, **84**, 930 (2006).

[43] R. Demirdag, E. Yerlikaya, M. Senturk, O.I. Kufrevioglu, C. Supuran. *J. Enzym. Inhib. Med. Chem.*, **28**, 278 (2013).

[44] E. E. Chufán, S. García-granda, M. R. Díaz, J. Borrás, J. C. Pedregosa. *J. Coord. Chem.*, **54**, 303 (2001).

[45] E. Bayram, M. Sentürk, O.I. Küfrevioğlu, C. Supuran. *Bioorg. Med. Chem.*, **16**, 9101 (2008).

[46] G. Shengli, L. Shengming, Y. Yuanqi, Y. Kaibei. *J. Coord. Chem.*, **46**, 145 (1998).

[47] Z. Alım, N. Kılınc, M.M. Isgör, B. Sengul, S. Beydemir. *Chem. Biol. Drug.*, **86**, 857 (2015).

[48] D. Ekinci, S.B. Ceyhun, M. Senturk, *D.* Erdem, O.I. Kufrevioglu, C.T. Supuran. *Bioorg. Med. Chem.*, **19**, 744 (2011).

[49] D. Ekinci, H. Cavdar, O. Talaz, M. Senturk, C.T. Supuran. *Bioorg. Med. Chem.*, **18**, 3559 (2010).

[50] M.I. Taskin, C. Bilen, A. Ergun, N. Gencer, U. Inceboz. *J. Chin. Med. Assoc.*, **78**, 513 (2015).

[51] I. Celik, H. Camas, O. Arslan, O.I. Kufrevioglu. *J. Environ. Sci. Health*, **31**, 2651 (1996).

[52] A.M. Vitale, J.M. Monserrat, P. Castilho, E.M. Rodriguez. *Comp. Biochem. Physiol. C*, **122**, 121 (1999).

[53] G. M. Sheldrick, SHELXS97 and SHELXL97, Programs for Crystal Structure Analysis, University of Göttingen, Göttingen, Germany, 1997.

[54] Stoe&Cie, X-Area (Version 1.18) and X-Red32 (Version 1.04), Stoe&Cie, Darmstadt, Germany, 2002.

[55] M.R. Gervais, B.L. Tufts. *Comp. Biochem. Physiol. A*, **23**, 343 (1999).

[56] M. Bulbul, O. Hisar, S. Beydemir, M. Ciftci, O.I. Kufrevioglu. *J. Enzyme Inhib. Med. Chem.*, **18**, 371 (2003).

[57] E. Dilek, S. Caglar. *Int. J. Pharm. Chem.*, **5(6)**, 189 (2015).

[58] E. Dilek, M.F. Polat. *Protein and Peptide Letters.*, **23**, 3 (2016).

[59] K. Nakamoto, Infrared and Raman Spectra of Inorganic and Coordination Compounds, Wiley, New York, 1986, pp. 230.

[60] C. Dendrinousamara, G. Tsotsou, L.V. Ekaterınıadou, A.H. Kortsarıs, C.P. Raptopoulou, A. Terzis, D.A. Kyriakidis, D.P. Kessissoglou. *J. Inorg. Biochem.*, **71(3-4)**, 171 (1998).

[61] F. Dimiza, F. Perdih, V. Tangoulis, I. Turel, D.P. Kessissoglou, G. Psomas. *J. Inorg. Biochem.*, **105(3)**, 476 (2011).

[62] M.R. Mendoza-Quijano, G. Ferrer-Sueta, M. Flores-Álamo, N. Aliaga-Alcalde, V. Gómez-Vidales, V.M. Ugalde-Saldívara, L. Gasque. *Dalton Trans.*, **41**, 4985 (2012).

[63] A. Biswas, L.K. Das, M.G.B. Drew, C. Diaz, A. Ghosh. *Inorg. Chem.*, **51**, 10111 (2012).

[64] E.H. Renata, M.B. Osório, A.P. Rosely, J.B. Adailton, R.A. Vicente, B. Szpoganicz, L.F. Franciele, T. Hernán, S.M. Antonio, M.M. Karen, E.C.F. Dalva, R.R. Willian, H. Wolfgang, T. Zbigniew, A. Ademir, N. Ademir. *Inorg. Chem.*, **51**, 1569 (2012).

[65] A. Neves, L.M. Rossi, A.J. Bortoluzzi, B. Szpoganicz, C. Wiezbicki, E. Schwingel. *Inorg. Chem.*, **41**, 1788 (2002).

[66] P. Bhowmik, L. K. Das, S. Chattopadhyay, A. Ghosh. *Inorg. Chim. Acta.*, **430**, 24 (2015). [67] C. Eicken, F. Zippel, K. Buldt-Karentzopoulos, B. Krebs. *FEBS Lett.*, **436**, 293 (1998).

[68] O. Ozensoy, O. Arslan, S. Sinan. *Biochemistry*, **69**, 216 (2004).

Figure Legends

Fig. 1. The molecular structure of the **1** showing the atom numbering scheme [symmetry code: (i) 1-x, 1-y, 1-z]

Fig. 2. 2D layer formed by π···π interactions of **1**.

Fig. 3. The molecular structure of the **3** showing the atom numbering scheme [symmetry code: (i) 1-x, 1-y, 1-z]

Fig. 4. The packing formed by C-H···π interactions of **3**.

Fig. 5. The molecular structure of the **4** showing the atom numbering scheme [symmetry code: (i) 1-x, 1-y, 1-z]

Fig. 6. 2D layer formed by C-Cl···π interactions of **4**.

Fig. 7. (a) Dependence of the reaction rates on $DTBCH_2$ concentrations for the oxidation reaction catalyzed by **3** and **4**. **(b)** Lineweaver-Burk plot for the catalysis by **3** and **4**.

Fig. 8. Determination of inhibition types and K_i values for the complexes using Lineweaver-Burk curves (for hCA I).

Fig. 9. Determination of inhibition types and K_i values for the complexes using Lineweaver-Burk curves (for hCA II).

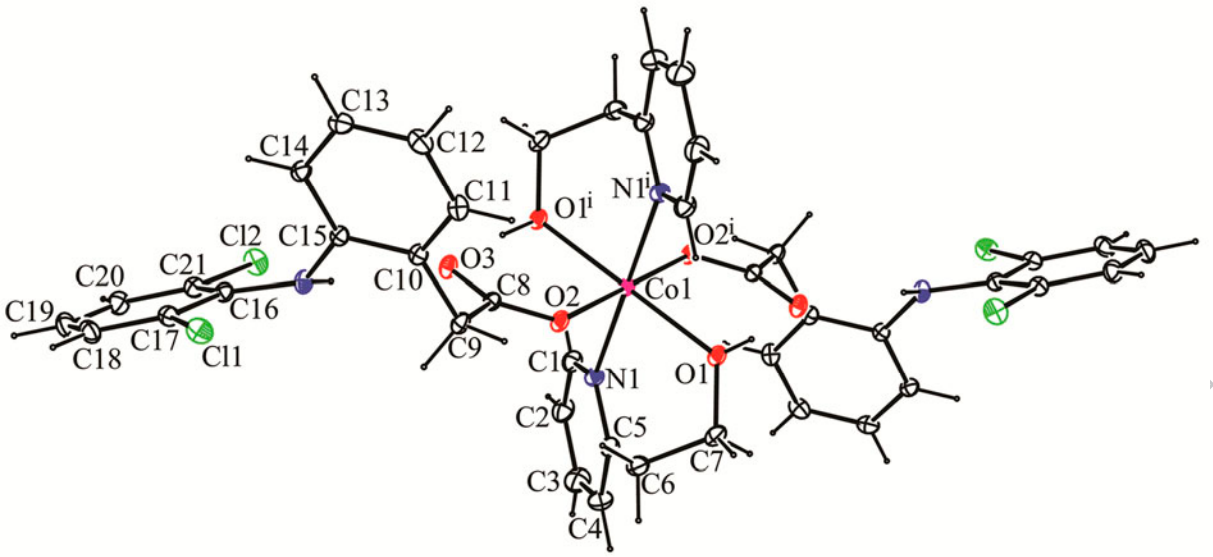

Fig. 1

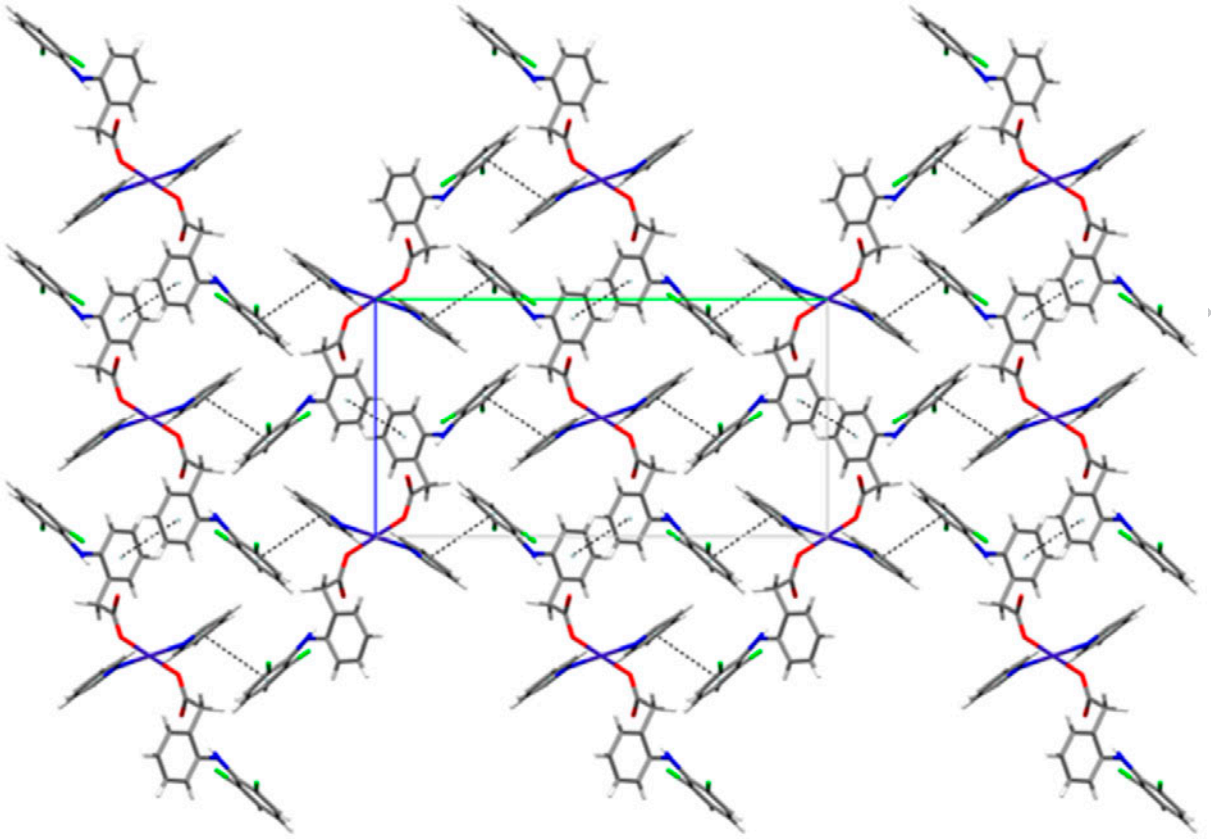

Fig. 2

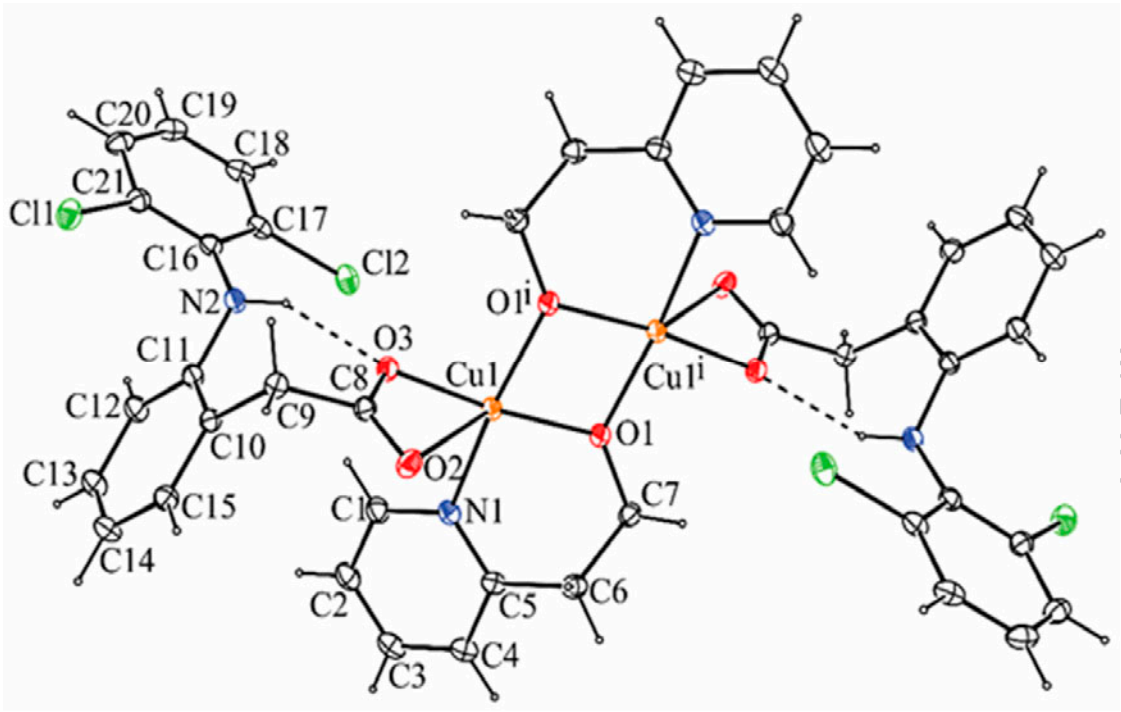

Fig. 3

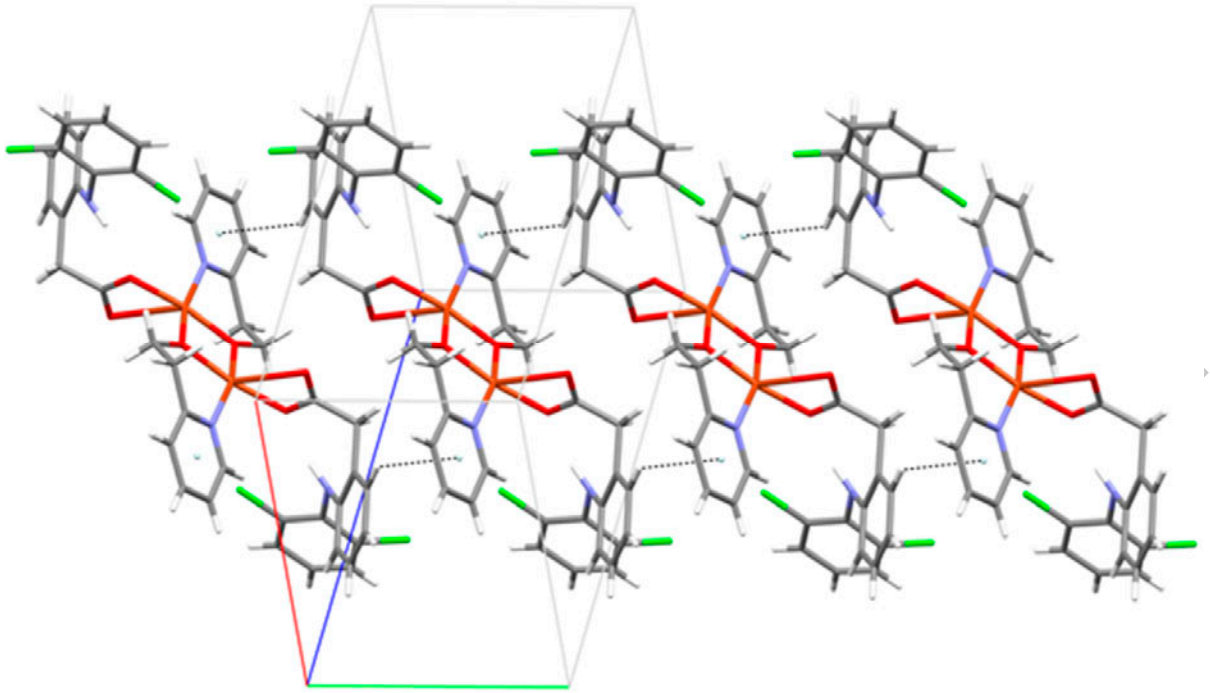

Fig. 4

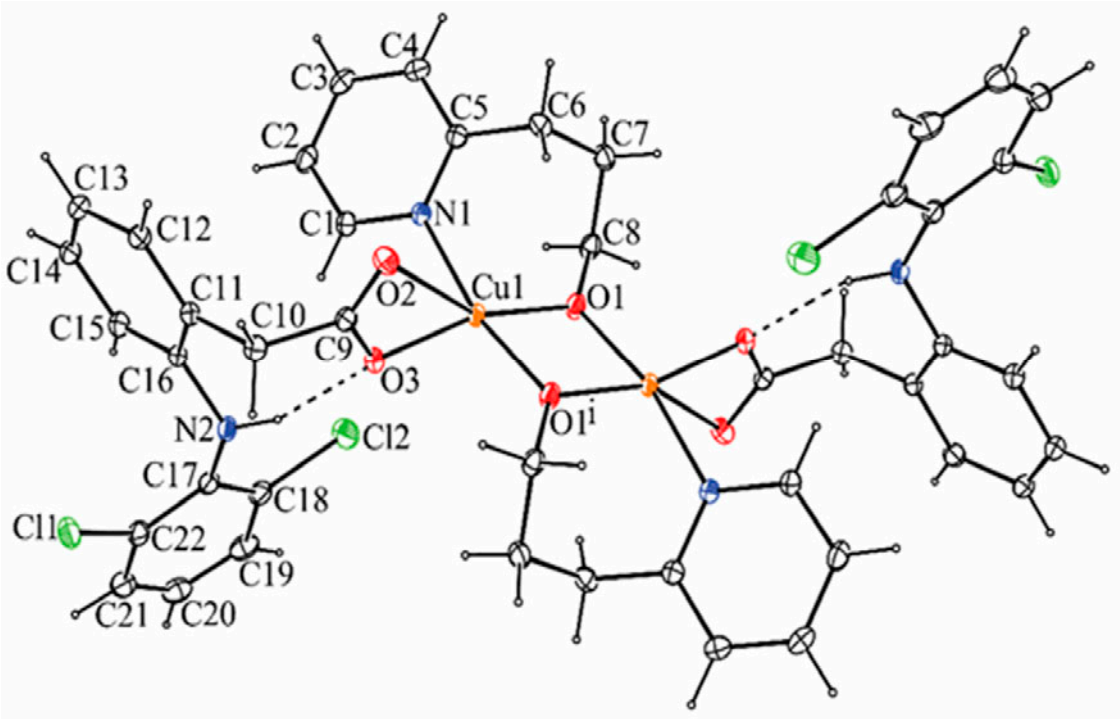

Fig. 5

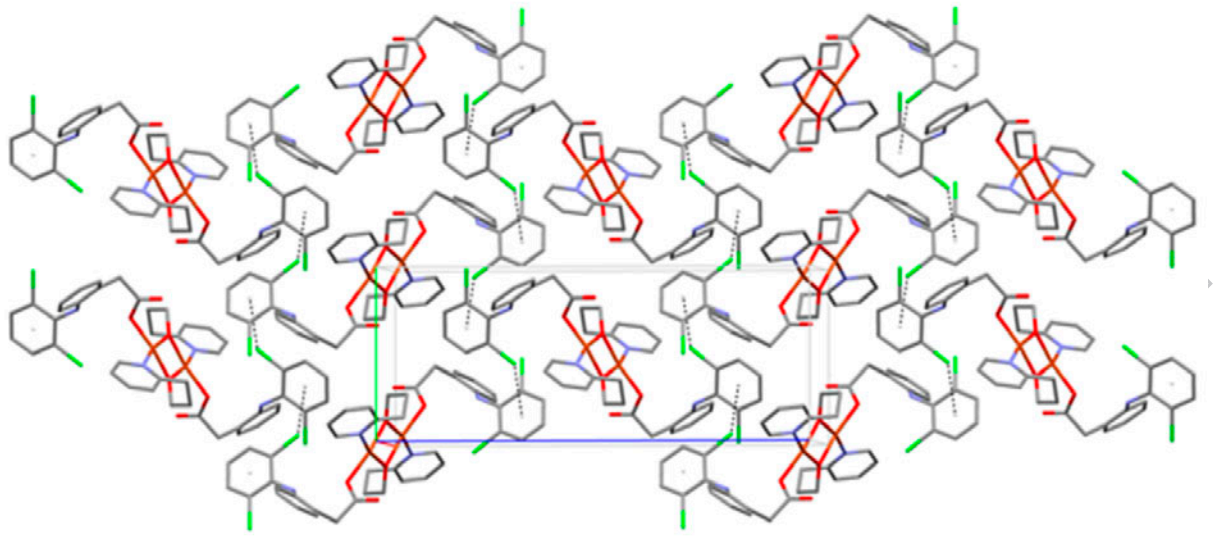

Fig. 6

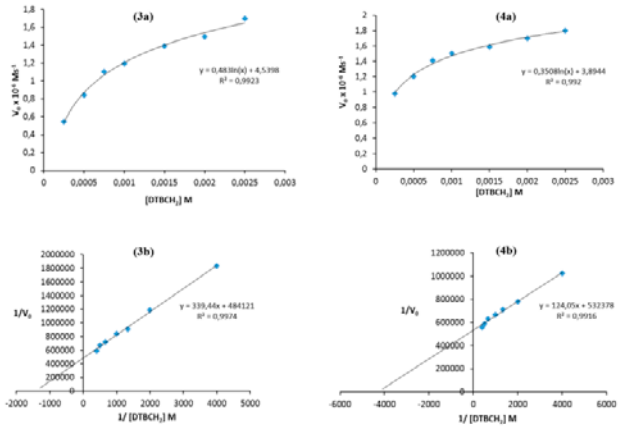

Fig. 7

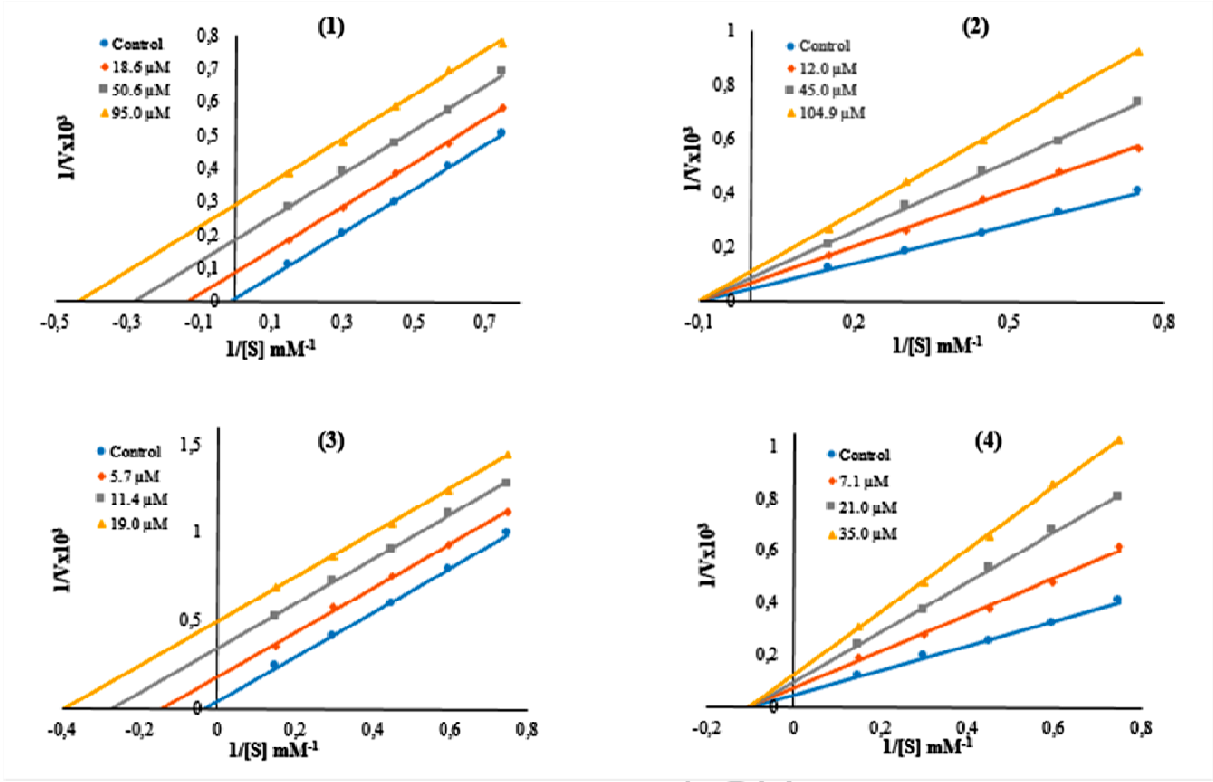

Fig. 8

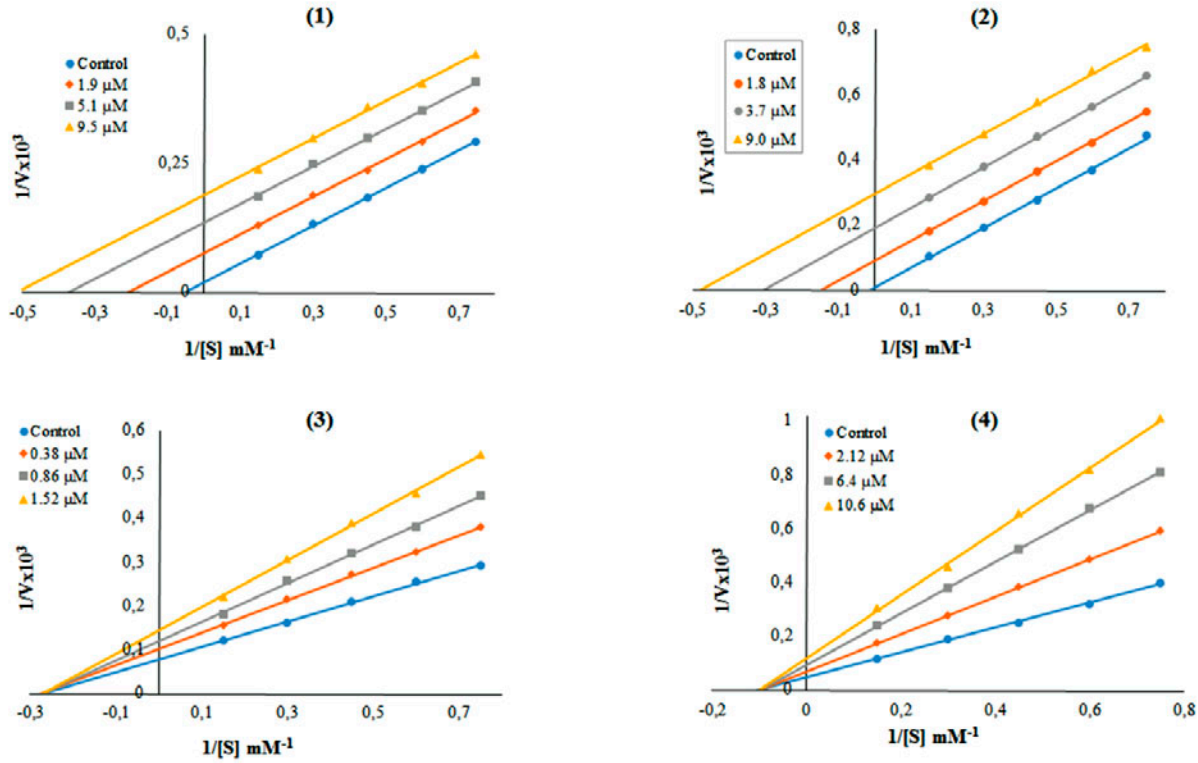

Fig. 9

Table 1. Crystal data and structure refinement parameters for **1**, **3** and **4**

	(1)	**(3)**	**(4)**
Empirical formula	$C_{42}H_{38}Cl_4N_4O_6Co$	$C_{42}H_{36}Cl_4N_4O_6Cu_2$	$C_{44}H_{40}Cl_4N_4O_6Cu_2$
Formula weight	895.49	961.63	989.73
Temperature (K)	293	293	293
Wavelength (Å)	0.71073	0.71073	0.71073
Crytal system	monoclinic	monoclinic	monoclinic
Space group	P21/c	P 21/c	P 21/c
Unit cell dimensions			
a (Å)	8.0798(3)	11.7479(5)	10.7735(4)
b (Å)	20.4071(7)	8.2759(2)	8.61585(23)
c (Å)	13.1154(5)	21.1225(9)	22.9349(8)
α (^{o})	90	90	90
β (^{o})	114.011(3)	99.815(3)	92.495(3)
γ (^{o})	90	90	90
V (Å)^3	1975.43(13)	2023.57(13)	2126.86(12)
Z	4	2	2
A. coefficient (mm^{-1})	0.76	1.369	1.305
D_{calc} (mg m^{-3})	1.506	1.578	1.5454
Crystal size (mm)	0.18; 0.42; 0.80	0.25;0.36;0.48	0.14; 0.42; 0.80
Theta range for data collection (^{o})	1.70;28.03	1.76;27.31	1.78;27.31
Measured reflections	22334	17369	27147
Indepen. reflections	11671	9880	12920
Absorpt. correction	Integration[a]	Integration[a]	Integration[a]
Refinement method	Full-matrix least-squares on F^2	Full-matrix least-squares on F^2	Full-matrix least-squares on F^2
Final R indices $[F^2 > 2\sigma(F^2)]$	0.0368	0.0454	0.0371
Goodness-of-fit on F^2	1.055	1.156	1.029

[a]Stoe and Cie (2002) [54]

Table 2. Selected bond distances (Ă) and angles (°) for **1, 3** and **4**

(1)			
Co1-N1	2.1340(17)	Co1-N1^{i}	2.1339(17)
Co1-O1	2.1320(13)	Co1-O1^{i}	2.1320(13)
Co1-O2	2.0934(13)	Co1-O2^{i}	2.0934(13)
O2-Co1-O1	89.50(5)	N1-Co1-N1^{i}	180.0
O2^{i}-Co1-O1	90.50(5)	O2-Co1-N1^{i}	85.39(6)
O1-Co1-O1^{i}	180.0	O1-Co1-N1^{i}	92.29(6)
O2-Co1-O2^{i}	180.0	O1^{i}-Co1-N1^{i}	87.71(6)
O2^{i}-Co1-N1^{i}	94.61(6)		
(3)			
Cu1-O1	1.906(2)	Cu1-N1	2.000(3)
Cu1-O1^{ii}	1.929(3)	Cu1-O3	1.921(2)
Cu1^{ii}-O1^{ii}	1.906(2)	Cu1^{ii}-N1^{ii}	2.000(3)
Cu1^{ii}-O1	1.929(3)	Cu1^{ii}-O3^{ii}	1.921(2)
Cu1-O2	2.739(3)		
O1-Cu1-O3	170.80(11)	O1-Cu1-N1	93.32(12)
O1-Cu1-O1^{ii}	76.76(12)	O3-Cu1-N1	95.49(12)
O3-Cu1-O1^{ii}	95.26(10)	O1^{ii}-Cu1-N1	163.42(12)
O1-Cu1-O2	124.88(9)	O3-Cu1-O2	53.11(9)
O1^{ii}-Cu1-O2	109.18(10)	O2-Cu1-N1	87.38(12)
(4)			
Cu1-O1	1.9159(19)	Cu1^{ii}-O1	1.9188(18)
Cu1-O1^{ii}	1.9188(18)	Cu1^{ii}-O1^{ii}	1.9159(19)
Cu1-N1	2.019(2)	Cu1^{ii}-N1^{ii}	2.019(2)
Cu1-O3	1.9240(18)	Cu1^{ii}-O3^{ii}	1.9240(18)
Cu1-O2	2.884(2)		
O1-Cu1-O3	162.79(8)	O1-Cu1-N1	96.50(9)
O1-Cu1-O1^{ii}	75.86(8)	O3-Cu1-N1	93.44(9)
O3-Cu1-O1^{ii}	96.44(8)	O1^{ii}-Cu1-N1	96.44(8)
O1-Cu1-O2	144.58(8)	O3-Cu1-O2	50.01(7)
O1^{ii}-Cu1-O2	94.37(7)	O2-Cu1-N1	86.32(8)

Symmetry codes: i:1-x,1-y,1-z; ii:1-x,-y,-z

Table 3. Geometric parameters of intermolecular interactions for **1**, **3** and **4** (Å,°)

D—H···*A*	*D*—H	H···*A*	*D*···*A*	*D*—H···*A*
(1)				
O1-H1A···O3^{i}	0.834(17)	1.778(18)	2.5801(19)	161(3)
N2-H2A···O3	0.878(15)	2.19(2)	2.929(2)	141(2)
C6-H6B···O2	0.97	2.382	3.146(3)	135
Ct1…Ct1^{ii}			3.8757	
Ct2…Ct3^{iii}			3.7681	
Ct3…Ct2^{iv}			3.7681	
(3)				
N2-H2A···O3	0.845(18)	2.11(3)	2.863(4)	148(3)
C15-H15…Ct1^{i}	0.93	2.86	3.5496	132
(4)				
N2-H2A···O3	0.842(17)	2.06(2)	2.834(3)	153(2)
C18-Cl2…Ct1^{i}	1.731(3)	3.5280(17)	4.626(3)	119.17(12)

(1) = (Ct1: C10/15; Ct2: N1C1/5; Ct3: C16/21; Symmetry codes: (i) 1-x, 1-y, 1-z; (ii) 1-x, 1-y, 2-z; (iii) x, 3/2-y, z-1/2; (iv) x, 3/2-y, z+1/2)

(3) = (Ct1: N1C1/5; symmetry code: (i) x, -1+y, z)

(4) = (Ct1: C17/22; symmetry code: (i) 1-x, 1/2+y, 3/2-z)

Table 4. IC_{50} values for the in vitro inhibition of hCA I and hCA II with synthesized complexes, by the esterase method with 4-NPA as substrate

Compound	IC_{50}(μM)	
	hCA I	hCA II
$[Co(dicl)_2(2\text{-}pyet)_2]$	60.36	5.79
$[Ni(dicl)_2(2\text{-}pyet)_2]$	54.62	4.58
$[Cu_2(dicl)_2(2\text{-}pyet)_2]$	10.83	0.85
$[Cu_2(dicl)_2(2\text{-}pypr)_2]$	20.39	5.78

Table 5. K_i values for the inhibition of hCA I and hCA II with synthesized complexes.

Compound	K_i (µM)		Inhibition type	
	hCA I	hCA II	hCA I	hCA II
$[Co(dicl)_2(2\text{-pyet})_2]$	1.91	0.89	noncompetetive	noncompetetive
$[Ni(dicl)_2(2\text{-pyet})_2]$	55.06	0.23	uncompetetive	noncompetetive
$[Cu_2(dicl)_2(2\text{-pyet})_2]$	1.52	1.54	noncompetetive	uncompetetive
$[Cu_2(dicl)_2(2\text{-pypr})_2]$	18.44	5.61	uncompetetive	uncompetetive